Titre: Title:	High-speed multinozzle additive manufacturing and extrusion modeling of large-scale microscaffold networks. Supplément
Auteurs: Authors:	Jean-François Chauvette, David Brzeski, Iee Lee Hia, Rouhollah D. Farahani, Nicola Piccirelli, & Daniel Therriault
Date:	2021
Type:	Article de revue / Article
Référence: Citation:	Chauvette, J.-F., Brzeski, D., Hia, I. L., Farahani, R. D., Piccirelli, N., & Therriault, D. (2021). High-speed multinozzle additive manufacturing and extrusion modeling of large-scale microscaffold networks. Additive Manufacturing, 47, 102294 (11 pages). https://doi.org/10.1016/j.addma.2021.102294

URL de PolyPublie: PolyPublie URL:	https://publications.polymtl.ca/49781/
Version:	Matériel supplémentaire / Supplementary material Révisé par les pairs / Refereed
Conditions d'utilisation: Terms of Use:	CC BY-NC-ND

Titre de la revue: Journal Title:	Additive Manufacturing (vol. 47)
Maison d'édition: Publisher:	Elsevier
URL officiel: Official URL:	https://doi.org/10.1016/j.addma.2021.102294
Mention légale: Legal notice:	

Supplementary information

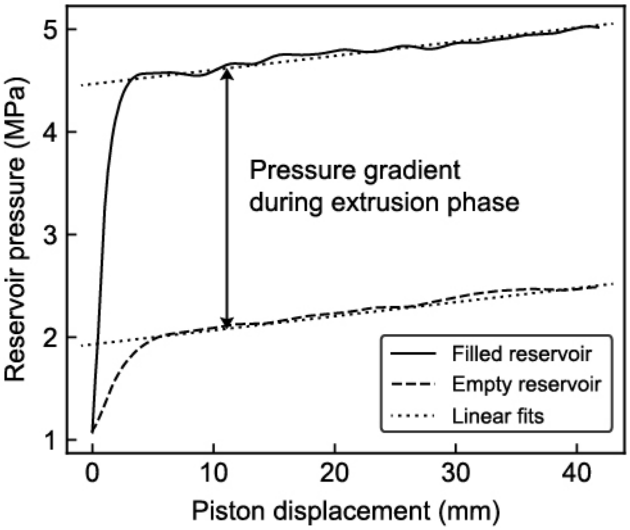

Figure S1. Measured pressure inside the multinozzle printhead for the extrusion of organic ink at 50 mm/s printing speed and the measured pressure for the empty reservoir at 50 mm/s printing speed (dry run), with respect to the same piston displacement. During the extrusion phase, the spring is compressed and applies a force on the cross-section area of the piston when the piston moves forward, constantly increasing the pressure in the hydraulic oil. The linear fit slopes exhibit the linear behavior of the spring, according to Hooke's law. The difference between the curves is mainly composed of the pressure gradient during material extrusion. Data was cleaned with a Gaussian filter (with standard deviation σ = 78 kPa).

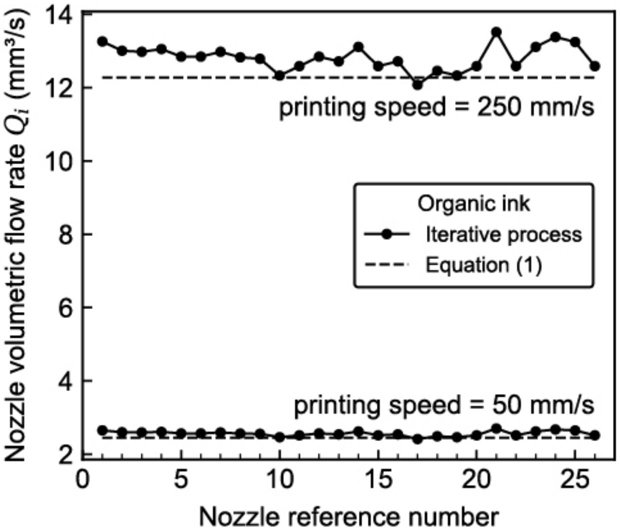

Figure S2. MEPM computation for individual nozzle volumetric flow rates using the organic ink at v = 50 and 250 mm/s for each nozzle of the multinozzle printhead. The resulting recalculated individual flow rates (Iterative process, solid line) diverge from to the first flow rate estimates (Equation (1), dashed line). The divergence is more significant at 250 mm/s (high printing speed) than at 50 mm/s (moderate printing speed).

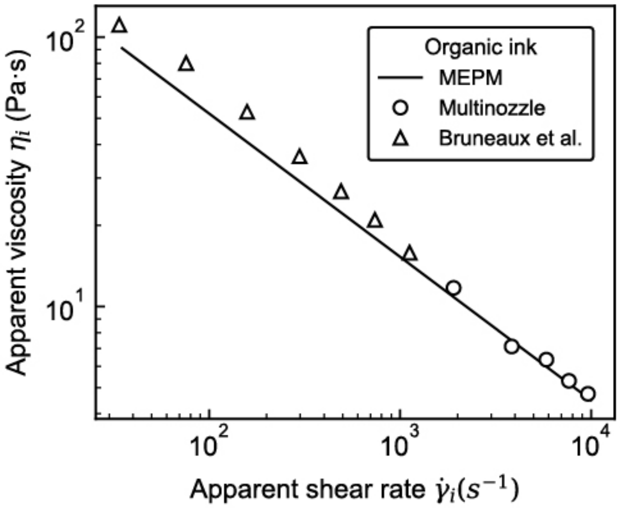

Figure S3. Viscosity as a function of the apparent shear rate calculation using the MEPM and experimental measurements for extrusion of organic ink (60/40 wt.%) using the multinozzle printhead ($\alpha = 26$, $D = 250$ µm, $L = 6.5$ mm). Results reported in [27] for single nozzle geometry ($\alpha = 1$, $D = 510$ µm, $L = 18.87$ mm) were superimposed for comparison.

v (mm/s)	**Average extruded mass (g)**	**Average extrusion time (s)**	**Mass flow rate (g/s)**	**Volumetric flow rate Q_{exp} (mm^3/s)[1]**
50	28	500	0.057	63.2
100	31	265	0.115	127.5
150	30	173	0.175	193.5
200	30	131	0.230	254.2
250	31	107	0.289	319.4

Table S1. Experimental volumetric flow rate calculation for printing speed v = 50, 100, 150, 200 and 250 mm/s.

[1] Using organic ink density $\rho_{\text{ink}} = 9.05 \times 10^{-4}$ g/mm^3 (estimated using the material components datasheet and ink composition)

Video S1. Case study #1: High-speed additive manufacturing of a large 5-layer microscaffold network (9 × 15 configuration, 225 mm × 375 mm × 1 mm) at 250 mm/s in ~1 minute 36 seconds (available at https://youtu.be/ZkN_StYn4uo).

Video S2. Case study #2: Multinozzle additive manufacturing of a 2-layer variable pore size microscaffold network (3 × 5 configuration) at 50 mm/s (available at https://youtu.be/xB34lHwUsog).